2022

# Towards New Antimalarial Drug: Depolarization of Liposomal Membranes by Aminooxoethylcarbamothioate in the Presence of Fe3+ Ions

Aaron Wilson

VCU logo

2022

# Towards New Antimalarial Drug: Depolarization of Liposomal Membranes by Aminooxoethylcarbamothioate in the Presence of $Fe^{3+}$ Ions

Aaron Wilson

Virginia Commonwealth University

# Towards New Antimalarial Drug: Depolarization of Liposomal Membranes by Aminooxoethylcarbamothioate in the Presence of $Fe^{3+}$ Ions

By

Aaron Wilson

PI: Dr. Vladimir Sidorov

Virginia Commonwealth University

Richmond, VA

May 2022

Acknowledgements

Thanks to everyone who helped make this research possible.

Table of Contents

List of Tables

Table Page

List of Figures

List of Abbreviations

| | |
|---|---|
| Acetonitrile | ACN |
| Ethyl Acetate | EtOAc |
| Dichloromethane | DCM |
| 8-Hydroxypyrene-1,3,6-trisulfonic acid | HPTS |
| Tetrahydrofuran | THF |
| Polytetrafluoroethylene | PTFE |
| Vapor Pressure Osmolality | VPO |
| Dynamic Light Scattering | DLS |
| Red Blood Cell | RBC |

Abstract

Towards New Antimalarial Drug: Depolarization of Liposomal Membranes by Aminooxoethylcarbamothioate in the Presence of $Fe^{3+}$ Ions

A thesis submitted in fulfillment of the requirements for the degree of Master of Science at Virginia Commonwealth University.

Virginia Commonwealth University, 2022.

Director: Vladimir Sidorov

Professor, Department of Chemistry

Despite the efforts of scientists around the world 409,000 people died of malaria in 2019 alone. According to the WHO 90% of those deaths occurred in Africa. Despite the high number of available treatments, malaria continues to plague many parts of the world. This is due in part to drug resistance developed among mosquito populations as well as limited access to medicines that do work. Furthermore, when traveling to malaria prone areas, pretreatment with a chemoprophylaxis is common practice. However, often the side effects to malaria pretreatment are severe. A new approach to the treatment of malaria is a compound that is only active in the presence of $Fe^{3+}$ ions and a negative transmembrane potential ($\Delta\psi$). In the parasitic stage where symptoms of malaria present, plasmodium falciparum invades erythrocytes and increases the concentration of free $Fe^{3+}$ in the cytosol of red blood cells. The novel compound 2-(naphthalen-1-ylamino)-2-oxoethyl) (2-bromoethyl) carbamothioate is shown to selectively lyse liposomes only under the presence of $Fe^{3+}$ and a transmembrane diffusion potential. These promising findings suggest a new type of malaria treatment that can depolarize and selectively kill *P. falciparum* during the erythrocytic cycle.

# Chapter 1

# Introduction

## 1.1 Malaria Overview

Malaria is a fatal disease caused by the *Plasmodium* parasites that are spread from the bite of an infected female *Anopheles* mosquito.[1] Of the more than 120 species of *Plasmodium*, five are known to infect humans. *Plasmodium falciparum* is the deadliest strain and the most prominent species in Africa while *P. vivex* is most prominent outside of Africa. However, Africa bears the largest burden of malaria infections and deaths. Of the 241 million cases and 627,000 deaths worldwide in 2020, 95% of cases and 96% of deaths originate from Africa. In Africa, children under 5 account for 80% of malaria related mortalities. To reduce the global impact of malaria, various strategies are employed. Vector control seeks to prevent the transfer of *Plasmodium* from the mosquito to the human host using insecticide-treated nets (ITNs) and indoor residual sprays. ITNs have the largest impact in high transmission areas, however their effectiveness is at risk due to increasing resistance to the pyrethroid insecticide by the *Anopheles* mosquito.[2] Efforts over the last 30 years to develop vaccines have been mostly unsuccessful. The first widely used vaccine was recommended for broad use by the WHO in September of 2021.[1] The vaccine showed significant protection over a 3-4-year period in older children with 36.3 % vaccine efficacy when given with a 20-month booster. However, the efficacy drops significantly in the much more at-risk group of very young children (6-12 weeks old at first dose).[3] Newer data also suggests that the vaccine does not provide even efficacy across all strains furthering the need for more novel drugs to combat the malaria crisis.[4] Chemoprophylaxis is the third strategy to prevent malaria infection. Various drugs such as doxycycline and atovaquone-proguanil are given to people traveling in malaria prone areas, nursing mothers, and young children. However, there are many variables to consider when

prescribing neurotoxic drugs as a chemoprophylactic. Therefore, more targeted drugs with fewer side effects are still sought after.

### 1.1.1 Biology of Infection

The life cycle of the *Plasmodium* parasite alternates between two vectors: the female *Anopheles* mosquito and vertebrate hosts. Within the vertebrate hosts, *P. falciparum* quickly moves from the blood stream to the liver where they invade and infect hepatocytes. Sporozoites within the blood stream transition from "migratory mode" to "invasive mode" upon recognition of cell surface proteins found on the surface of hepatocytes. Upon recognition sporozoites enter the host cell and form a parasitophorous vacuole in which they develop. While developing within the hepatocytes they undergo schizogony until tens of thousands of daughter merozoites are released in budding packets of merosomes into the vasculature.[5] Once in the vasculature free merozoites invade erythrocytes in a fast, multi-step process that is complete within 2 minutes. After infection of the erythrocytes is established, each merozoite undergoes a second round of schizogony, producing 16-32 merozoites that release from the RBC, destroying the cell membrane in the process. These merozoites are then free to infect more erythrocytes. In a process that is still not well understood, some merozoites within erythrocytes transition from making more asexual merozoites to form male and female gametocytes. It is these male and female gametocytes that are necessary to complete the transmission from humans back to mosquitoes after a female *Anopheles* mosquito takes a blood meal during this stage.

### 1.1.2 Drug Resistance

Drug resistance in malarial parasites has become a growing problem around the world. Chloroquine, the most widely used and successful drug to treat malaria, is no longer the miracle drug it used to be. In central Africa's Democratic Republic of the Congo, researchers attributed the rise in both cases and mortality to the increasing resistance to chloroquine.[6] From 1982 to 1986 the proportional malaria

admission rate increased from 29.5% to 56.4% and the proportional malaria mortality rate increase from 4.8% to 15.3%. In 1982 there were no cases of in vivo or in vitro chloroquine-resistant malaria in the African city of Kinshasa. By 1986, 82% of *P. falciparum* isolates exhibited drug resistance in vitro, suggesting that the rise in hospital admission rates and mortality rates were directly due to this increase in resistance.[7] Other treatments, such as sulfadoxine-pyrimethamine, were used in areas of Africa where resistance to chloroquine was high. However, resistance to this drug therapy was also developed in *P. falciparum* isolates after treatment .[8] While countless researchers have examined the ways in which *Plasmodium* becomes resistance to new drugs, the fact remains that until effective vaccines are in broad use, new anti-malarial drugs used for both treatment and chemoprophylaxis are in high demand.

### 1.1.3 Iron Metabolism

During the erythrocytic cycle of infection, merozoites undergo rapid cell division to produce approximately 16-32 new merozoites. This process is energy intensive and requires a constant source of fuel. Lucky for the parasite, it just happens to be within reach of a steady source of amino acids in the form of hemoglobin. Hemoglobin represents about 95% of the soluble protein within the RBC, at a concentration of 340 mg/mL.[9] Radiolabeled amino acids within hemoglobin have been shown to be incorporated within parasite proteins.[10] However, it has also been shown that hemoglobin amino acids serve a nonanabolic process as well. A significant portion of those amino acids are excreted by the intraerythrocytic parasite. It has been proposed that either the parasite is making room for itself or controlling the RBC osmotic stability.[11,12] In either case, the merozoite ingests the hemoglobin through an invagination of the parasitophorous vacuolar and parasite plasma membrane called the cytostome. The hemoglobin is transported through this opening into an acidic food vacuole for degradation. Many proteases are involved in breaking down hemoglobin and targeting these proteases with inhibitors has been a strategy for antimalarial drug development. This has been met with limited success, likely due to the redundant functions of proteases.[9] After hemoglobin has been digested within the acidic vacuole,

the byproduct is free heme groups. As free heme is toxic to the cell due to oxygen radical catalysis, it has to be sequestered in the form of hemozoin. Hemozoin is an inert crystal that removes the iron moiety from solution chemistry.[13] This crystalline pigment was associated with a malaria infection as early as 1849.[14] Disrupting the formation of hemozoin crystals within the parasitophorous vacuole has been the target of many antimalarials. The antimalarial quinolines such as chloroquine, quinine, and mefloquine work by inhibiting the formation of hemozoin, leading to the toxic buildup of heme.[15] These compounds work by passively diffusing through the cell membrane and into the acidic digestive vacuole. Once in the acidic vacuole the weakly basic amine groups on the quinolines become protonated, conferring a positive charge on the compound and effectively trapping it within the vacuole. Trapped within the vacuole where the degradation of hemoglobin occurs, it is able to inhibit the formation of hemozoin leading to the toxic buildup of heme. Paradoxically *Plasmodia* has to synthesize its own heme rather than use the heme broken down from its host.[16] In fact, the demand for iron for the parasite is quite high as iron is used for DNA synthesis, glycolysis, heme synthesis, etc. Therefore, *Plasmodia* needs access to a labile iron pool, that is bioavailable iron is chelatable and redox active. It is still under debate as to where the major source of this iron comes from[17]. However, researchers have shown that as the parasitic cycle within the erythrocyte progresses, the labile iron pool increases. Because the need for access to the labile iron pool is necessary for the parasite's replication, it is viewed as a potential target for antimalarials. Iron chelation has already been shown to inhibit erythrocytic *Plasmodium* in vitro and in vivo.[18] Iron chelators work by either withholding necessary iron from *Plasmodia* or by forming toxic complexes with iron. In this work the latter case is examined, in which the iron chelated complex is lethal to the *Plasmodium*.

### 1.1.4 Intro of Novel Carbamothioate

In this study, the efficacy of the novel compound 2-(naphthalen-1-ylamino)-2-oxoethyl) (2-bromoethyl) carbamothioate is assessed for the treatment of malaria. The carbamothioate has two unique properties that could make it a potential antimalarial therapeutic drug; It is an amphipathic molecule with a nonpolar naphthalene group that should be able to cross a semipermeable membrane and its polar tail has several sites that could chelate with iron. One potential conformer is illustrated in Figure 1 in which $Fe^{3+}$ could chelate with lone pairs on either of the carbonyl groups or the sulfur atoms. However, there are also lone pairs on both amine groups as well so other conformations that would allow iron chelation likely exist.

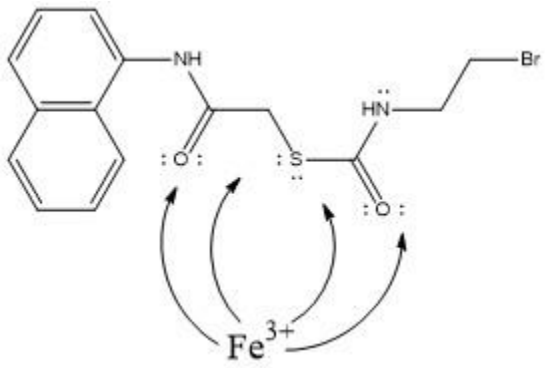


Figure 1. Potential $Fe^{3+}$ chelation sites with the carbamothioate.

In an erythrocyte infected with malaria, this compound should diffuse through the RBC membrane and chelate with $Fe^{3+}$. Once chelation occurs, the compound would then carry a net positive charge, attracting it to the negatively charged cell membrane of *P. falciparum*. The nonpolar naphthalene tail of the compound could then insert itself into the cell membrane of *P. falciparum* causing depolarization and cell lysis and therefore parasite death. Because this compound should only work in the presence of free $Fe^{3+}$ and be attracted to a negatively charged membrane, it should be highly selective. Furthermore, the resting transmembrane potential of a plasmodia parasite is approximately -90 mV while for an

erythrocyte it's only -10 mV[19, 20]. This large difference in potentials offers yet another avenue of selectivity to potentially exploit. To test whether this novel compound could depolarize a cell membrane under both a transmembrane potential and in the presence of $Fe^{3+}$ ions, liposomes were used as a model for the *Plasmodia* parasite. Liposomes were made with an internal buffer containing a high concentration of potassium relative to the external buffer they are suspended in so that a negative transmembrane potential could be generated using a selective potassium transporter. They were also prepared with an internal dye, HPTS, used to monitor the integrity of the liposomes. Two primary assays were used in assessing the liposome integrity. First, Safranin O was used to determine whether a transmembrane potential can be applied across the membrane of the liposome, and secondly, whether the liposomes hold up under that transmembrane potential. The transmembrane potential was generated using valinomycin. Valinomycin, shown in Figure 2, is a selective potassium transporter that diffuses freely through lipid membranes.

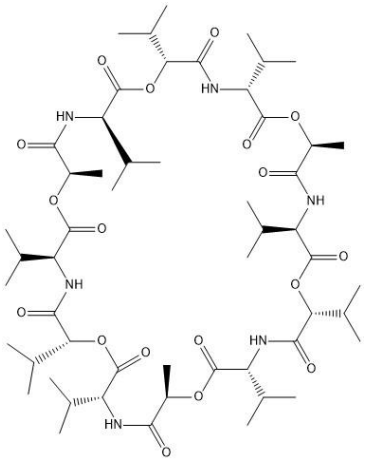

Figure 2. Structure of Valinomcyin.

Valinomycin contains a pore in the center that is over 10,000 times more selective for potassium ions than sodium.[21] Since the internal buffer contains a higher concentration of potassium relative to the external buffer, valinomycin transports the potassium down its concentration gradient to the external

buffer generating a negative transmembrane potential. To measure this potential, Safranin O is used. Safranin O works by changing the intensity of its absorbance as a function of a transmembrane potential.[22] Safranin O has been shown to stack upon induction of a transmembrane potential and that results in a spectral shift that is linearly related to a transmembrane potential. Using the spectral shift of Safranin O, one can monitor the development of a transmembrane potential generated by valinomycin and determine how stable the liposome is under those conditions. However, due to fluorescent quenching of Safranin O by iron, the depolarization experiments in the presence of iron were not compatible with Safranin O. Instead, HPTS was used to indirectly measure depolarization of liposomes. HPTS, shown in figure 3, is a pH sensitive dye that has two unique fluorescent signatures from its unprotonated and protonated forms. This allows one to change the pH of the external buffer and monitor the liposome structural integrity as a function of those pH changes. As the HPTS dye is within the liposome, changes to the pH should not affect the internal dye in stable liposomes.

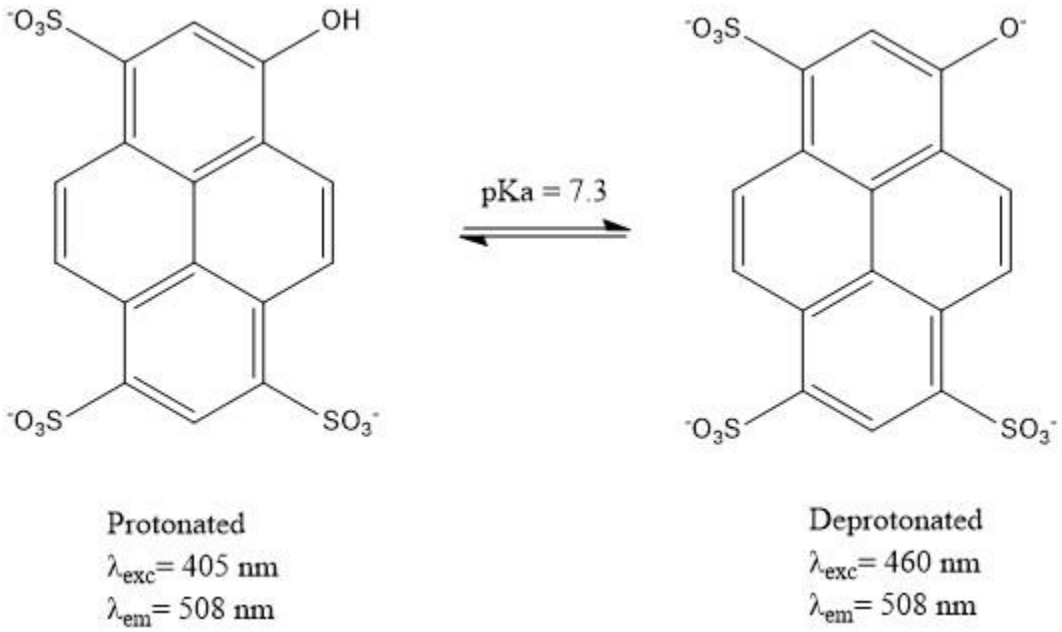


Figure 3. Fluorescent dye HPTS.

# Methodology

## 2.1 Compound Synthesis

The following synthesis is depicted in figure 4 below. 210 mg of 1-napthylisothiocynante were added to a 100 mL round bottom flask. To the flask, 12 mL of acetonitrile was added and the mixture was stirred until dissolved. To the flask, 70 µL of ethanolamine were added and the mixture was stirred with a magnetic stir bar for approximately 4 hours. Then 120 µL of triethylamine were added and stirred for approximately 10 minutes. After this time the flask was put on ice. An addition of 103 µL of bromoacetylbromide was mixed with 2 mL of acetonitrile and put on ice until chilled. This mixture was then very slowly added to the flask and allowed to stir on ice for approximately 4 hours. This mixture was heated at reflux at 75 ° C for approximately 4 hours. After reflux, the flask was allowed to cool and placed on a rotovap to remove solvent. The crude was weighed and dissolved in approximately 2 mL of 87:13 DCM:EtOAc. A sample of crude was submitted to LC-MS analysis before purification. The crude was then purified on a packed silica gel column using 87:13 DCM:EtOAc as eluent. The purified product was collected in fractions, tested via TLC, and then all fractions containing the compound of interest were combined. The combined purified product was then dried to a neat material, weighed, and then tested via NMR for purity.

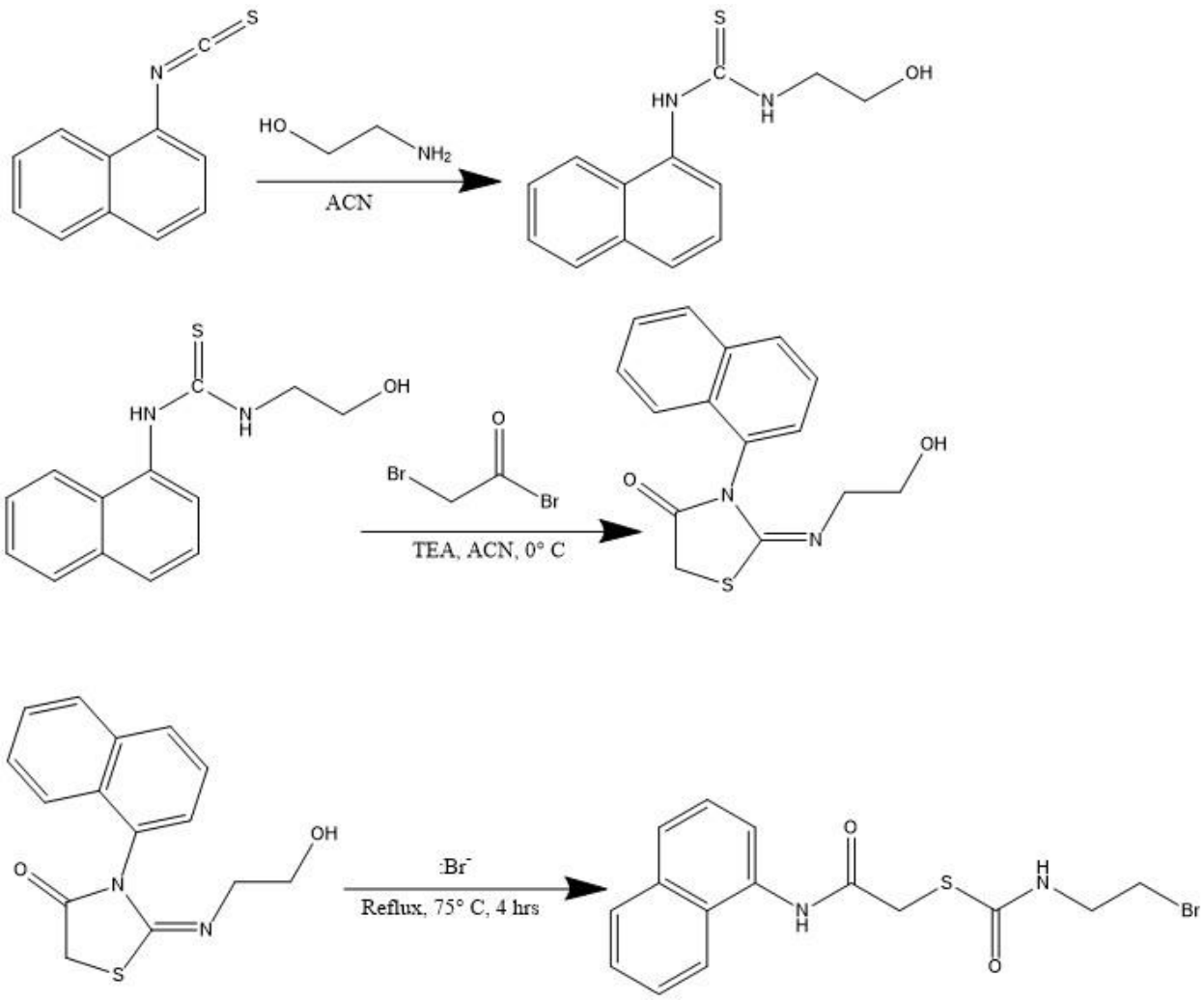


Figure 4. Synthetic Scheme

2.2 Solution Preparation

- Buffer A (pH 6.4, 100 mM NaCl): 0.8824 g of $NaH_2PO_4$, 0.3761 g of $Na_2HPO_4$, and 5.8405 g NaCl were added to a 1 L volumetric flask and diluted to volume with type 1 water.
- Buffer B (pH 6.4, 100 mM KCl): 0.8827 g of $NaH_2PO_4$, 0.3757 g of $Na_2HPO_4$, and 7.4508 g KCl were added to a 1 L volumetric flask and diluted to volume with type 1 water.
- 100 µM HPTS dye: 192 mgs of HPTS were added to a 10 mL volumetric flask and diluted to volume with buffer B. A 683 µL aliquot of this solution was then added to a 25 mL volumetric flask and diluted to volume with buffer B.

- Triton-x25: Triton-x100 was diluted 1:4 with DI water
- 3.75 µM Valinomycin in DMSO: 20 mgs of valinomycin were diluted into 25 mL of DMSO. Then a 521 µL aliquot was diluted to 10 mL with DMSO.
- 0.5 M $NaOH_{(aq)}$: 0.1120 g of NaOH was dissolved into 5.6 mL of Type 1 water.

2.3 Liposome Synthesis

Egg yolk L-α-phosphatidylcholine (EYPC ethanol solution, 120 µL, 79 µmol) was dissolved in chloroform/methanol solution, evaporated under reduced pressure until a thin lipid cake coated all sides of the round bottom flask. It was then dried under high vacuum for 2 hours. The lipid film was then hydrated with 1,200 µL of 100 µM HPTS dye in buffer B. Seven freeze/thaw cycles were performed using a dry ice acetone bath and a 50 °C water bath. The resulting suspension was subjected to 21 high-pressure extrusions through a 0.1 µm polycarbonate membrane at room temperature. Through size-exclusion chromatography (SEC) using G-75 Sephadex, the extra-vesicular buffer with HPTS was replaced with buffer A to a concentration of 11 mM.

2.4 Fluorometric experiments:

All fluorometric measurements were performed at 15 °C using a Flouromax 3 (Jobin-Yvon/Horriba) spectrophotometer.

2.4.1 Safranin O potential buildup:

Liposomes were diluted in buffer A containing 60 nM Safranin O to a liposome concentration of 550 µM and placed in a quartz cuvette under gentle stirring. Fluorescent emission was monitored at 580 nm with excitation at 520 nm. At 100 seconds the cuvette was spiked with 20 µL of 3.75 µM valinomycin. At 800 seconds 20 µL of buffer B was spiked into the cuvette. The fluorescence was monitored until 1000 seconds.

### 2.4.2 8-Hydroxypyrene-1,3,6-trisulfonic acid (HPTS) Experiments:

HPTS experiments were conducted by diluting the liposomes into buffer A to make a liposome concentration of 550 µM. The excitation wavelengths for the protonated and unprotonated HPTS were set at 405 nm and 460 nm respectively and both emission wavelengths were monitored at 508 nm. If iron was added, 62.5 µL of 0.5 mM $FeCl_3$ in buffer A was added before the run. If added, 20 µL of 3.75 µM valinomycin in DMSO was added at 60 seconds. Either DMSO for blanks or our compound was spiked at varying concentrations noted in Table 1 at 200 seconds. In fluorimetry experiments 26.3 µL of 0.5 M NaOH is added. Finally, 50 µL of triton-x25 is added at 600 seconds. Emission spectra is recorded until 800 seconds.

To convert the raw data of both traces (protonated HPTS and deprotonated) the response of deprotonated HPTS is divided by protonated. This gives a ratio of deprotonated to protonated HPTS. The average is then normalized to zero using data from 0-59 seconds as this is before the addition of any compounds and sets the baseline to zero. The maximum ratio is then normalized to 100 by dividing each response by the maximum response and multiplying by 100. This sets the baseline to zero and the maximum response ratio to 100. This allows each run to be compared more accurately.

Table 1. Spiking regime for HPTS fluorescence

| Run | 0.5 mM $FeCl_{3\,(aq)}$ | Valinomycin 3.75 µM | Drug/DMSO |
|---|---|---|---|
| Double Blank | - | - | 50 µL DMSO |
| No Fe, no Val | - | - | 10 µM drug |
| Val, no Fe | - | 62.5 µL | 10 µM drug |
| Fe, no Val | 62.5 µL | - | 10 µM drug |
| Fe and Val | 62.5 µL | 62.5 µL | 10 µM drug |

2.5 Vapor Pressure Osmometry (VPO) analysis:

VPO analysis was performed by weighing out $FeCl_3$ and our compound. Each was diluted to the concentrations noted in Table 2 in and Table 3. A 10 µL aliquot of sample was added onto a filter paper that was then inserted into the Wescor VAPRO analyzer and analyzed for vapor pressure. Prior to analysis the VPO was calibrated with premade stock $NaCl_{(aq)}$ standards at 100, 270, and 1,000 mmol/kg. Microosmolality was calculated by dividing the weight of the sample by the molecular weight, multiplying the number of ions that compound generates (1 for carbamothioate and 4 for $FeCl_3$) and multiplying by 100,000.

2.6 Dynamic Light Scattering (DLS) studies:

DLS studies were conducted using a Malvern Zetasizer ZS. Sample were weighed and diluted in 70:30 THF:$H_2O$. They were then filtered through a 0.45 PTFE filter, sonicated, and aliquoted into a quartz cuvette and placed within the Zetasizer. All samples were equilibrated for 5 minutes prior to DLS measurements and conducted at 25 °C. Carbamothioate was prepared at 4 mg/mL in all runs for a concentration of 11 mM. $FeCl_3$ was prepared at 24.15 mg/mL for a concentration of 150 mM.

## Results and Discussion

### 3.1 Compound synthesis.

Before the sample was purified via silica column chromatography, a 5 mg sample was submitted to the MassSpec department at VCU for LC-MS analysis. The total ion chromatogram in Figure 5 shows two prominent peaks at m/z 389 and 391. These peaks represent the decyclized product with a sodium adduct$[M+22]^+$. Two peaks are present because the compound contains bromine at equal isotopic abundances. Two peaks of compound are also present at 405 and 407 in which it is forming an adduct with potassium, $[M+39]^+$. The peak at 287, [M+1] represents the other isomer from step 2 of the synthesis. This product cannot undergo decyclization and is separated upon silica column chromatography. After purification the compound was tested via NMR as shown in figure 6 and compared to values obtains from Franklin, C., et al. illustrated in Figure 7.[23] As each chemical shift in the NMR in figure 6 matched the literature NMR that was obtained from Dr. Constance Franklin, it was determined that the compound had been successfully synthesized and purified.

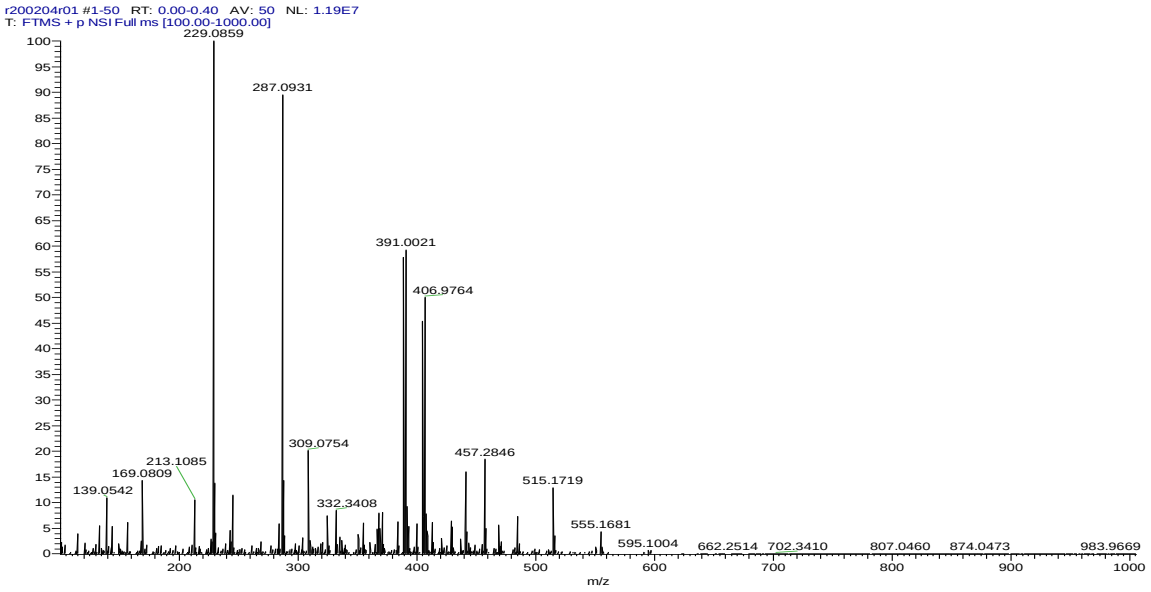


Figure 5. TIC of crude from synthesis prior to silica column chromatography.

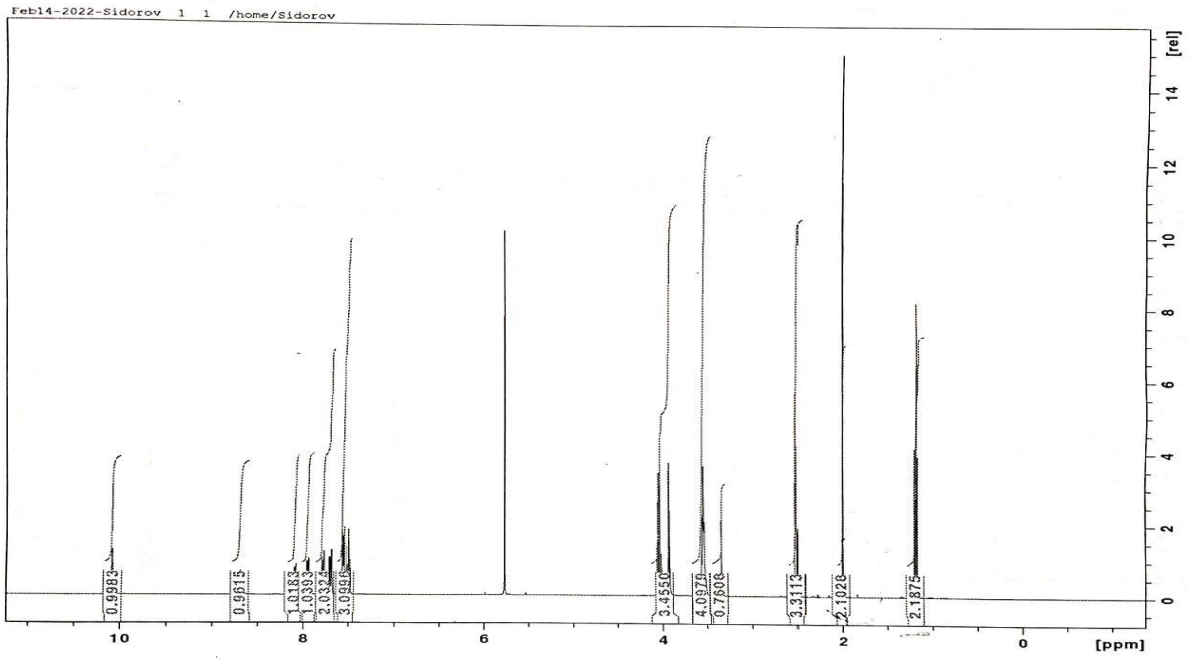


Figure 6.$^{1}$H NMR of carbamothioate in DMSO-$d_6$ at 400 MHz

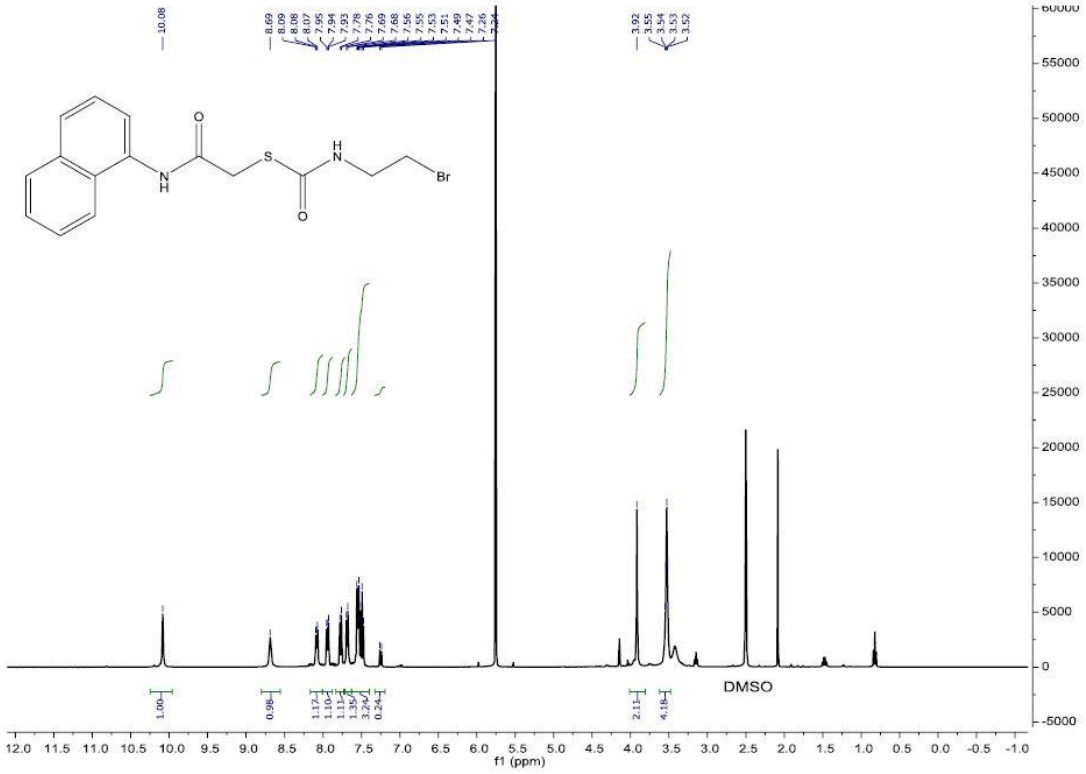


Figure 7. Literature $^{1}$H NMR of carbamothioate in DMSO-$d_6$ at 400 MHz

## 3.2 Liposome potential induction measured by Safranin O

In this study liposomes were used to model the conditions of a *Plasmodia* parasite within an infected erythrocyte. The conditions the carbamothioate would target the membrane were with free $Fe^{3+}$ in solution and a negative transmembrane potential. However, to first determine the capacity of the liposomes to generate a potential in the presence of valinomycin, Safranin O was used. Safranin O, as shown in Figure, 8 is a cationic dye that without the positive charge would be hydrophobic. However, due to that positive charge on the tertiary amine, the compound is water soluble. When in solution with a lipid membrane the Safranin O stays in the aqueous phase. Then when a negative charge potential is generated across the lipid membrane, the Safranin O partitions into the hydrophobic membrane and starts to stack. This stacking results in an increase in emission intensity that is directly related to the charge applied across the membrane. As illustrated in Figure 9, when the selective potassium transporter valinomycin is added to solution, the emission spectra spikes. Because the concentration of $K^+$ is higher inside the liposome, when the valinomycin is added, it captures $K^+$ ions and shuttles it down its concentration gradient to the extravesicular solution generating a negative transmembrane potential. The equilibrium between charge and concentration is quickly met and the potential remains consistent until the addition of potassium buffer.

Two important pieces of information were concluded from this experiment. First, the liposomes were able to generate a potential across the lipid membrane. Secondly, after that initial buildup of charge, the slope of the intensity remains at zero. This illustrates that the liposomes are stable under the transmembrane potential that is generated. Later experiments seek to perturb the liposomes and determining that valinomycin and a transmembrane potential alone aren't enough to cause liposomal lysis is necessary to validate those experiments.

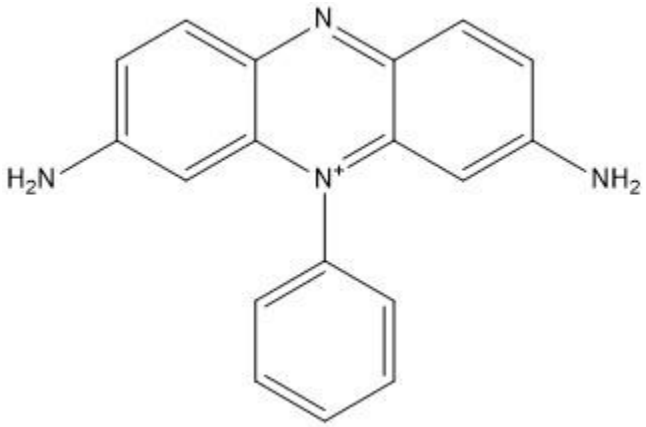


Figure 8. The cationic dye Safranin O.

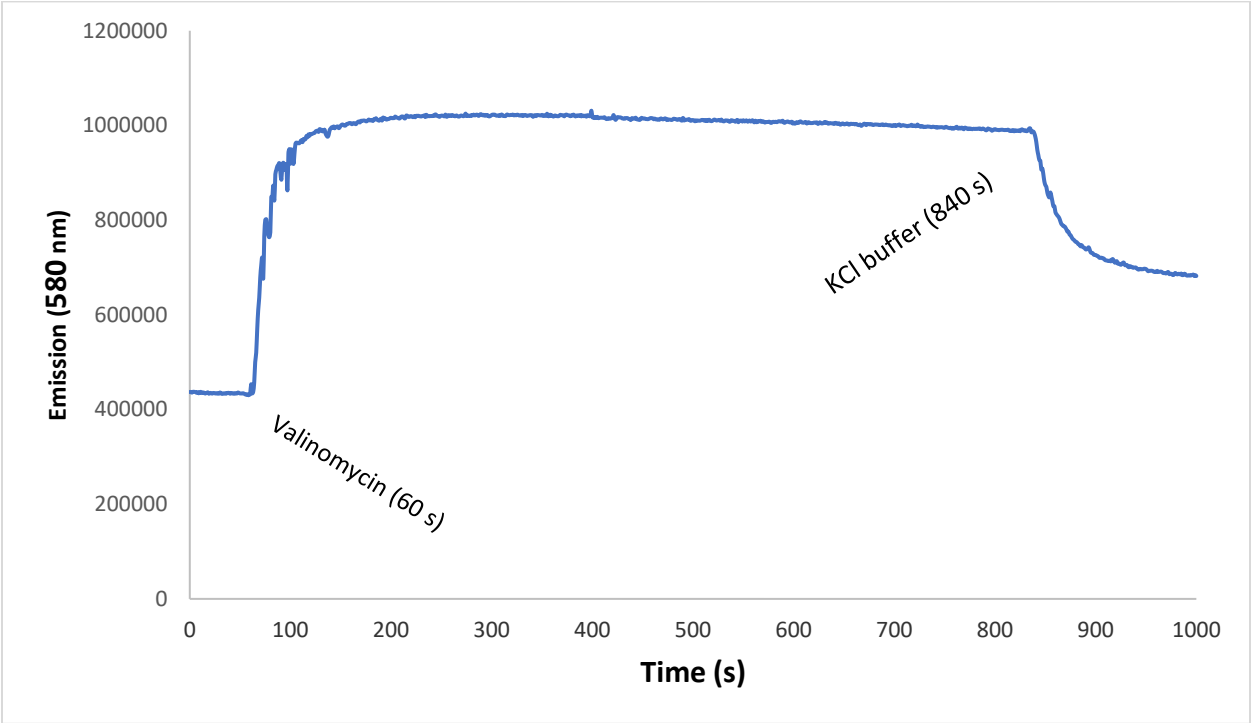


Figure 9. Liposomes with internal KCl buffer suspended in extravesicular NaCl buffer. $\lambda_{exc}$ = 520 nm, $\lambda_{em}$ = 580 nm. At 60 seconds the selective $K^+$ transporter valinomycin is added. At 840 seconds external KCl buffer is added.

## 3.3 Results from HPTS fluorometry.

The HPTS fluorescent dye within the liposome was used to indirectly measure the liposome integrity. As intravesicular dye within the liposome should not be affected by changes to the pH of the extravesicular solution, so any amount of deprotonation events can be seen as the liposomes becoming less stable and/or undergoing lysis. This allows one to determine if the carbamothioate is able to effectively destabilize and/or depolarize the liposomes under certain conditions.

A typical double blank run, as shown in figure 10, starts with liposomes with intravesicular HPTS dye and KCl buffer suspended in dye-free NaCl buffer. Both protonated and deprotonated HPTS fluorescence are monitored in the spectrophotometer. At this point the intravesicular and extravesicular pH is 6.4 and the baseline is set to 0. DMSO is spiked into the cuvette at 200 seconds with minimal changes in the baseline. At 300 seconds 26.3 µL of 0.5 M $NaOH_{aq}$ is added. In all experimental runs, including the blanks, some amount of HPTS is deprotonated. However, when compared to other experimental runs, the level of deprotonation remains constant as illustrated by the flat lines between 300 seconds and 600 seconds in which trition-x25 is added. At 600 seconds, upon the addition of the surfactant triton, all liposomes lyse and release the intravesicular dye exposing it to the basic solution and causing the ratio of deprotonated to protonated HPTS to reach its maximum value. Therefore, to compare the efficacy of the carbamothioate, the amount and rate of deprotonation events that occur between 300 and 600 seconds is compared between experiments. The yellow trace in Figure 10 that represents the double blank with no $FeCl_3$, no valinomycin, and DMSO shows the flattest baseline between 300 and 600 seconds illustrating the least amount of deprotonation events. The grey trace in which carbamothioate is present at 10 µM does increase slightly, indicating a slight capacity to perturb the liposomal membrane without either a transmembrane potential or free $Fe^{3+}$. This is also seen in the run (dark blue)

in which valinomycin is added without iron indicating slight activity in the presence of membrane potential alone. However, as the membrane potential of plasmodia is much higher than the erythrocyte in which it is inhabiting, this still favors the carbamothioate to target the parasite. The orange trace, in which $FeCl_3$ is present without valinomycin also shows depolarization potential indicating that iron chelation alone is sufficient to generate compound activity. However, the trace with the steepest slope, indicating the highest deprotonation rate, is the run in which both iron and valinomycin are present shown in the light blue trace in Figure 10. This suggests that the novel compound is able to most effectively target the membrane in conditions that are most similar to those found within a malaria infected erythrocyte. The fluorimetry study in Figure 11 illustrates another promising property of the compound, dose dependency. In this example, both the double blank (DMSO without valinomycin) and the blank (DMSO with valinomycin) exhibit flat baselines between 300 and 600 seconds. However, as the concentration of carbamothioate is increased, the rate of deprotonation increases. With each increasing dose, not only does the total amount of deprotonated HPTS increase, the slope of the line between 300 and 600 seconds also increases. This illustrates a clear dose-dependent response.

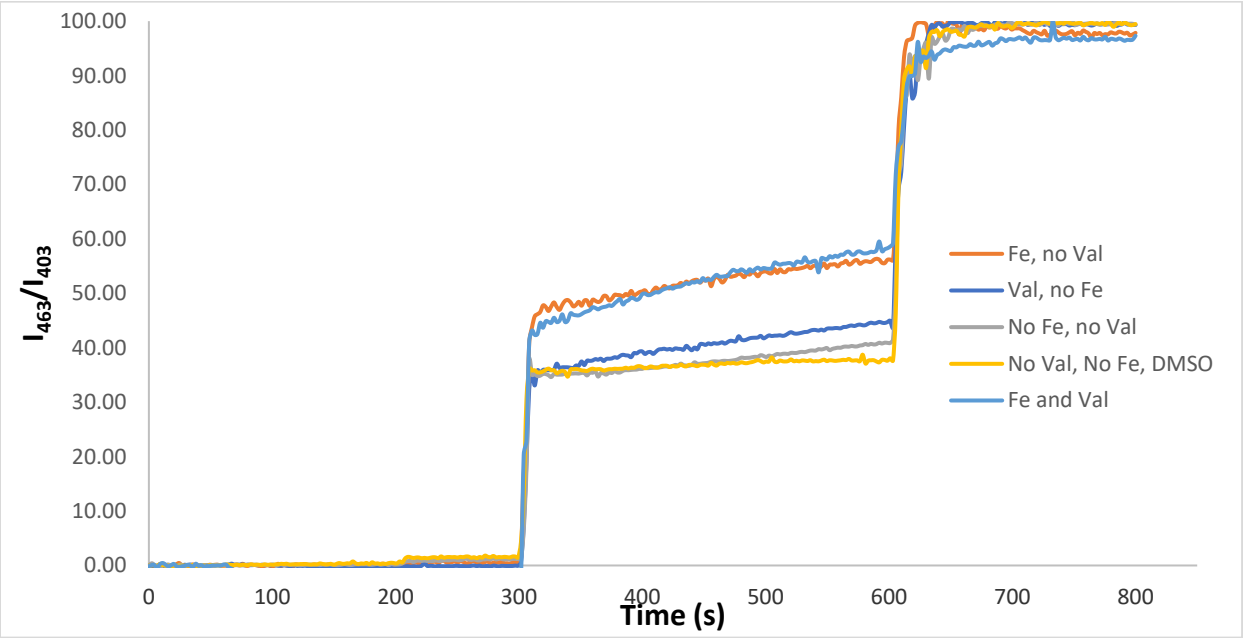


Figure 10. Liposome integrity monitored with and without valinomycin, $Fe^{3+}$, and carbamothioate.

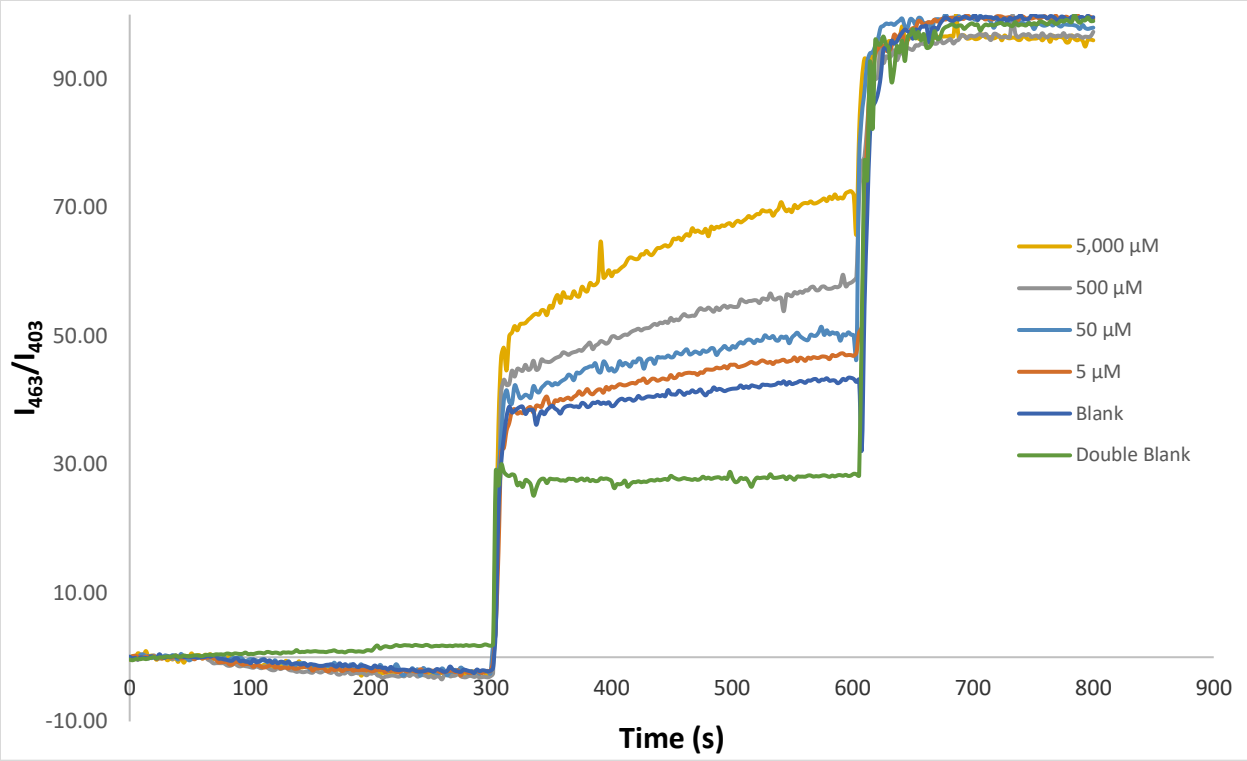


Figure 11 Dose dependent response monitored by HPTS fluorescence.

3.4 Vapor Pressure Osmolality.

The VPO results shown in Figures 12-14 were used to determine the relationship between $Fe^{3+}$ and the carbamothioate. Based off the structure of the compound it was hypothesized that it would chelate with iron. Using that information, it was hypothesized that the vapor pressure of a solution containing both iron and carbamothioate would be less than the sum of individual solutions of iron and carbamothioate. Vapor pressure is a colligative property based solely on the number of individual solutes in a solution. If $Fe^{3+}$ and the compound chelate together in solution that reduces the total number of solutes and therefore the vapor pressure should be less than the respective sums of the $Fe^{3+}$ and compound alone. To test this, three solutions at differing concentrations of $FeCl_3$ and compound were analyzed via VPO in a solution of 90:10 THF:$H_2O$. The results of the individual readings were then used to calculate the theoretical vapor pressure of a solution containing both carbamothioate and $FeCl_3$ assuming no

interaction/chelation. This was done by subtracting the solvent blank vapor pressure from the vapor pressure results of either $FeCl_3$ or compound alone. An example calculation for the theoretical vapor pressure of a solution containing both $FeCl_3$ and carbamothioate is illustrated in Equation 1.

$VPO_{theo}=(FeCl_3\ VPO_{raw}-\text{Solvent}) + (\text{Carbamothioate}\ VPO_{raw}-\text{Solvent}) + \text{Solvent}$ Equation 1

Using this formula, one can determine what the theoretical vapor pressure of a solution containing both $FeCl_3$ and carbamothioate if they do not interact and exist as individual solutes in solution. Results of raw VPO and theoretical vapor pressure calculations are shown in Table 2. These values were then plotted in Excel using microosmolality on the x-axis and the instrument vapor pressure reading in mmol solute/kg of solvent on the y-axis. As shown in Figure 12, there was an enhanced instead of reduced response when the VPO was taken of both $FeCl_3$ and the carbamothioate.

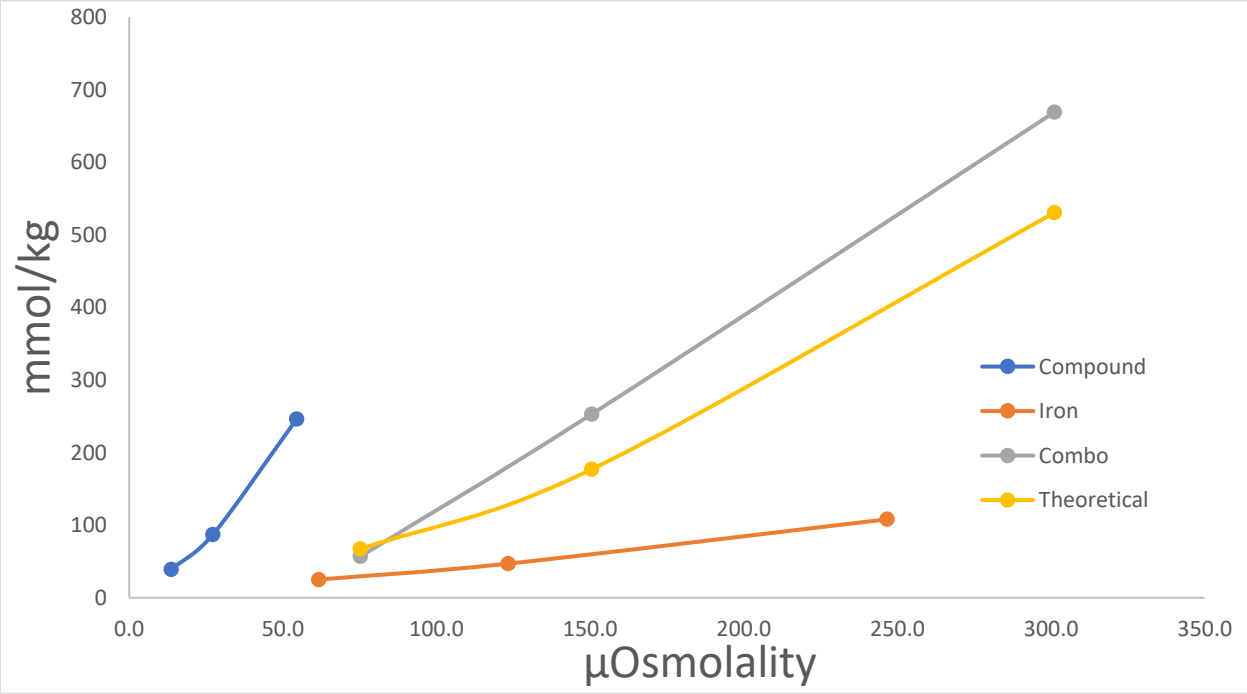


Figure 12. VPO of $FeCl_3$, carbamothioate, combination, and theoretical in 90:10 THF:$H_2O$

Table 2. VPO values for compound, iron, combination, and theoretical in 90:10 THF:$H_2O$

| Iron (µsol/mL) | Compound (µsol/mL) | $VPO_{raw}$ (mmol/kg) | $VPO_{Cor}$ (mmol/kg) | $VPO_{Theo}$ (mmol/kg) |
|---|---|---|---|---|
| - | - | 76 | 0 | - |
| - | 54.5 | 322 | 246 | - |
| - | 27.2 | 163 | 8 | - |
| - | 13.6 | 115 | 39 | - |
| 247 | - | 184 | 108 | - |
| 123 | - | 123 | 47 | - |
| 61.6 | - | 101 | 25 | - |
| 54.5 | 247 | 745 | 669 | 430 |
| 27.2 | 123 | 329 | 253 | 210 |
| 13.6 | 61.6 | 133 | 57 | 140 |

One potential explanation was that there was not enough water in the 90:10 THF:$H_2O$ solution and that iron was experiencing limited solubility. It was surmised that when mixed with the carbamothioate it enhanced the solubility of the $FeCl_3$, increasing the number of solutes in solution, thereby increasing the vapor pressure reading. To test this, the experiments were repeated in a solution of 70:30 THF:$H_2O$ to ensure full solubility of the $FeCl_3$. This solution presented its own unique problems; Increasing the concentration of carbamothioate did not result in an increasing vapor pressure and there was still an enhanced vapor pressure greater than the sum of each individual solution as shown in Figure 13.

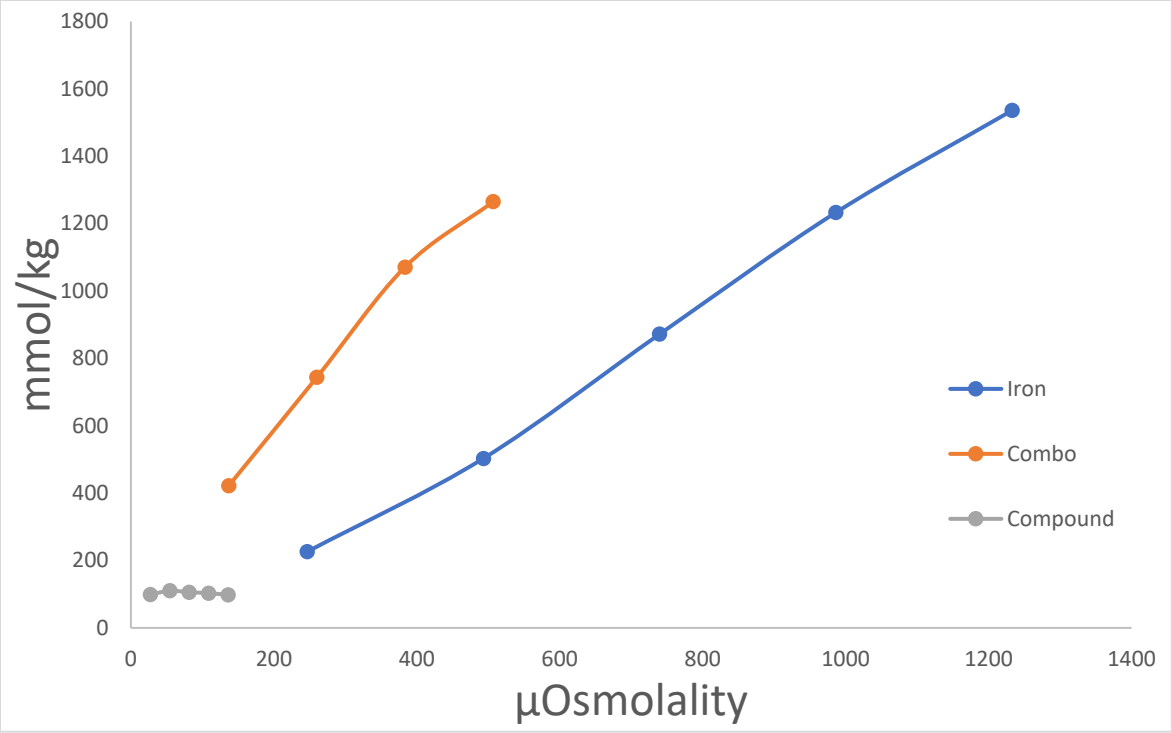


Figure 13. VPO of $FeCl_3$, carbamothioate, and combination in 70:30 THF:$H_2O$.

The compound was fully solubilizing as there was no turbidity or cloudiness in solution and as the increasing concentration of iron resulted in a clear linear increase in vapor pressure, the limited solubility theory didn't hold up. It was then hypothesized that the compound was forming micelles in the THF:$H_2O$ mixtures. This would explain no increases in vapor pressure reading as the compound concentration increases. The total number of individual solutes would not increase as concentration increases if they are congregating in micelles. Also, the enhanced vapor pressure reading when in combination with the $FeCl_3$ can also be explained with micelle formation. If the compound does indeed chelate $Fe^{3+}$, then the micelles that formed would be disrupted by the $Fe^{3+}$ in solution. As the $Fe^{3+}$ chelates with the polar tail of the compound, the accumulating positive charge on the micelles would begin to repel each other, causing the micelle to break apart, increasing the number of individual solutes

in solutions and thereby increasing the vapor pressure. To test this hypothesis, the vapor pressure of compound was tested at a steady concentration while increasing the concentration of iron only. Those same concentrations of $FeCl_3$ that were used in combination with the compound were then individually tested at those exact concentrations and subtracted from those values from the combination of both $FeCl_3$ and compound. Raw vapor pressure values from these experiments are described in Table 3. In this way, one can determine that the vapor pressure was increasing as a result of the increase in $Fe^{3+}$ concentration, even after correcting for the contribution from that the $FeCl_3$. As shown in Figure 14, this was true at all four concentrations of compound. In all cases, increasing the iron concentration resulted in increased vapor pressure. This was attributed to the micelles breaking down with each addition of $FeCl_3$. To begin to characterize the size and formation of potential micelles, VPO experiments were not enough.

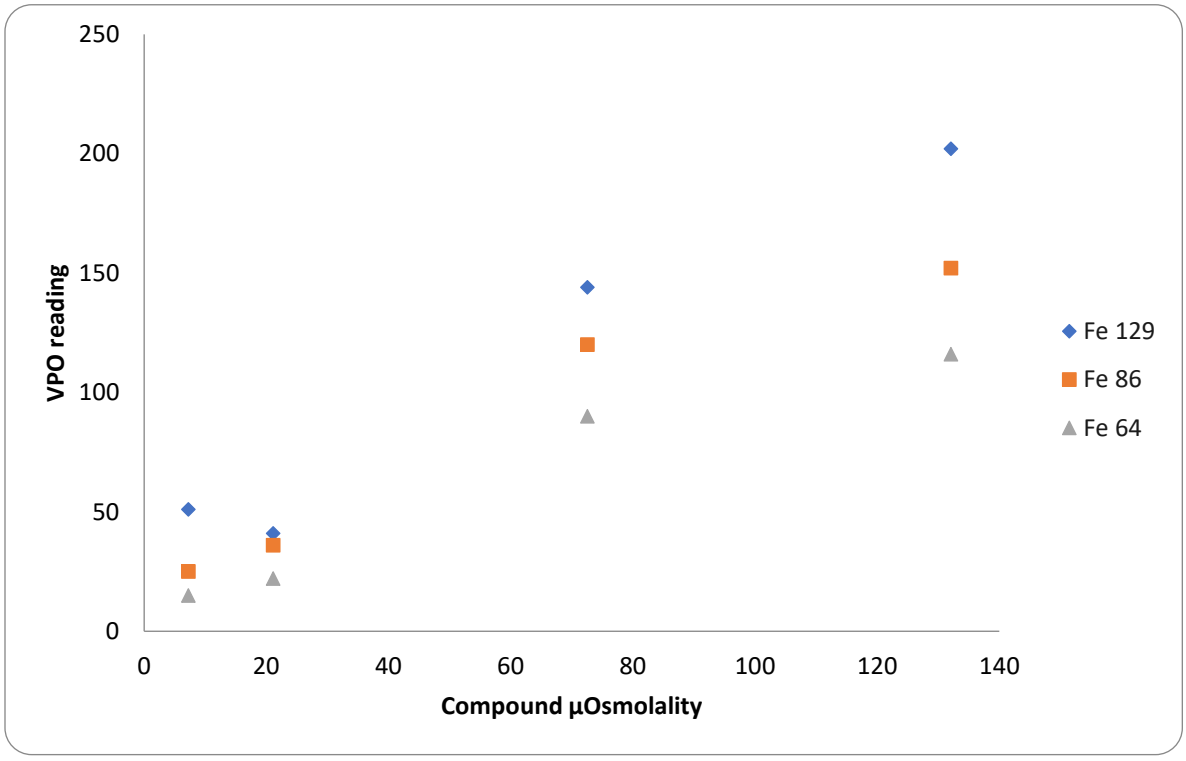


Figure 14. VPO of compound at various $FeCl_3$ concentrations.

Table 3. VPO values of carbamothioate with varying Fe concentrations

| Iron (µsol/mL) | Compound (µsol/mL) | $VPO_{raw}$ (mmol/kg) | $VPO_{Cor}$ (mmol/kg) |
|---|---|---|---|
| 128 | - | 101 | - |
| 85.8 | - | 95 | - |
| 64.4 | - | 95 | - |
| 128 | 7.26 | 152 | 51 |
| 85.8 | 7.26 | 120 | 25 |
| 64.4 | 7.26 | 110 | 15 |
| 128 | 21.1 | 142 | 41 |
| 85.8 | 21.1 | 131 | 36 |
| 64.4 | 21.1 | 117 | 22 |
| 128 | 72.6 | 245 | 144 |
| 85.8 | 72.6 | 215 | 120 |
| 64.4 | 72.6 | 185 | 90 |
| 128 | 132 | 303 | 202 |
| 85.8 | 132 | 247 | 152 |
| 64.4 | 132 | 211 | 116 |

### 3.5 Dynamic Light Scattering

The VPO experiments strongly suggested the formation of micelles. However, to confirm their presence, dynamic light scattering (DLS) was used to determine the particle size of potential micelles. The solvent blank in Figure 15 shows just one peak at approximately 7 nm. This peak shows up in all of the DLS experiments and is likely an artifact of the THF:$H_2O$ solvent. When looking at the compound in solution at 4 mg/mL there is another peak at approximately 700 nm illustrated in Figure 16. This peak potentially represents the micelles forming in solution**.** However, because larger particles scatter light much more than smaller particles, the peak at 700 nm is present in much lower concentrations than the peak at 6.5 nm as the intensity of scattering of a particle is proportional to the sixth power of its diameter[24]. If these are the micelles of the carbamothioate, then the VPO data suggests that adding $FeCl_3$ would cause those

micelles to break apart and the peak at 700 nm to go away. To look at the outcome of adding the $FeCl_3$ to the carbamothioate solution the DLS of $FeCl_3$ was first taken. Figure 17 shows the same peak present in all samples plus an additional peak at approximately 100 nm. As this doesn't overlap with the potential micelle peak at 700 nm the DLS particle size measurements of compound with varying amount of $FeCl_3$ were able to be conducted. As shown in Figures 18 and 19, as the concentration of $Fe^{3+}$ in solution increases, the peak at approximately 700 nm decreases in intensity until it goes away all together. This strongly supports the theory that the compound is indeed forming micelles and that these micelles break up in the presence of $Fe^{3+}$. This makes perfect sense, as the concentration of $Fe^{3+}$ increases, more and more $Fe^{3+}$ ions chelate with the compound on the surface of the micelle. As these positive charges accumulate, the coulombic repulsion is greater than the intermolecular bonds keeping the micelle together and the newly chelated Fe-carbamothioate complex breaks away from the micelle until the micelle is fully broken apart.

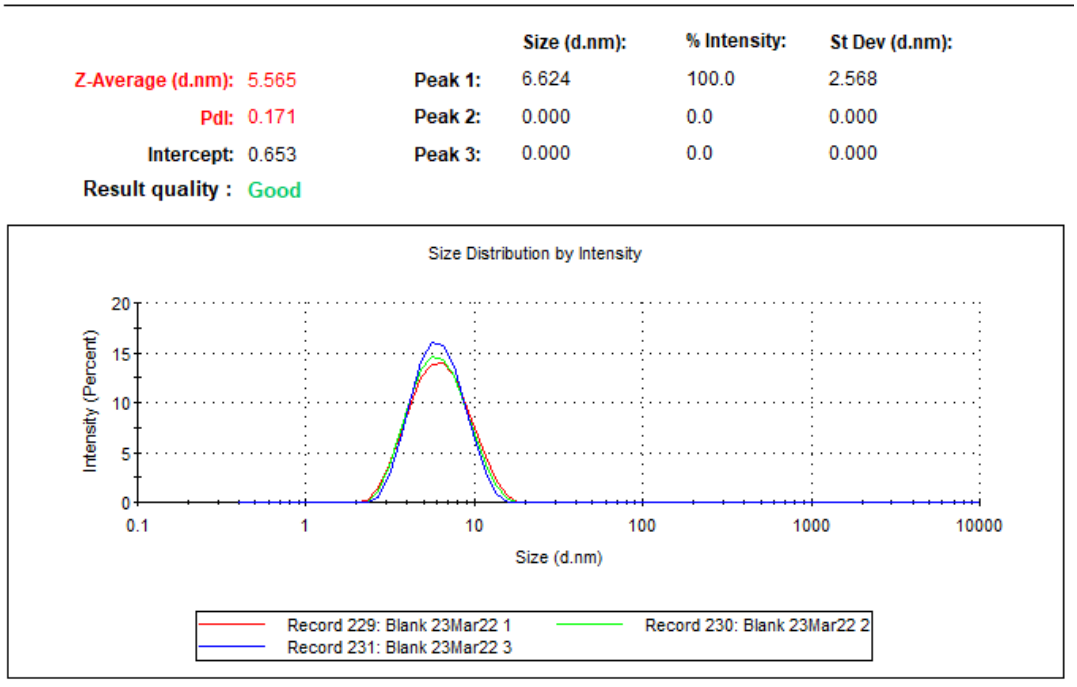


Figure 15. DLS of Solvent blank (70:30 THF:$H_2O$).

| | | | Size (d.nm): | % Intensity: | St Dev (d.nm): |
|---|---|---|---|---|---|
| Z-Average (d.nm): | 11.65 | Peak 1: | 6.453 | 72.1 | 1.720 |
| PdI: | 0.311 | Peak 2: | 709.0 | 27.9 | 321.8 |
| Intercept: | 0.679 | Peak 3: | 0.000 | 0.0 | 0.000 |

**Result quality :** Refer to quality report

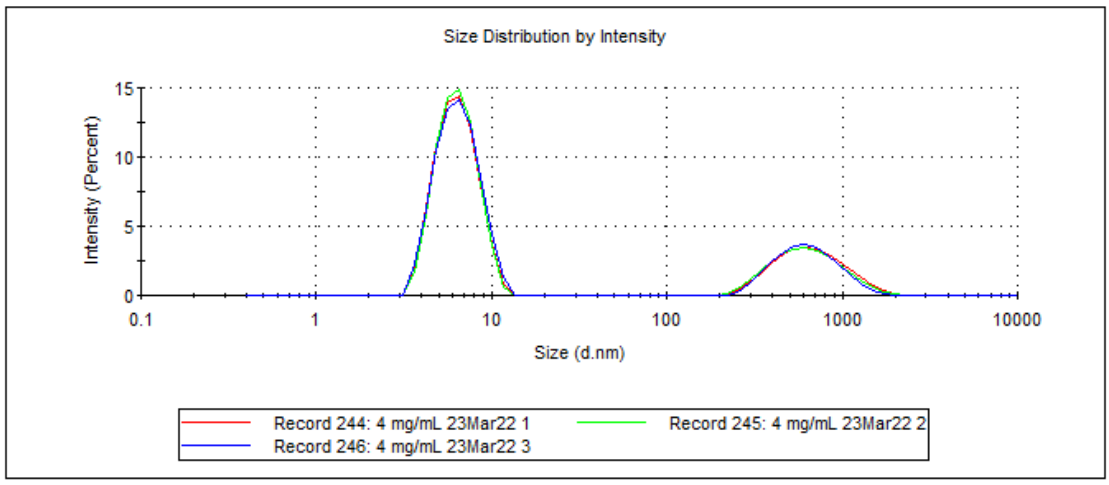


Figure 16. Carbamothioate in 70:30 THF:$H_2O$ at 11 mM.

| | | | Size (d.nm): | % Intensity: | St Dev (d.nm): |
|---|---|---|---|---|---|
| Z-Average (d.nm): | 38.73 | Peak 1: | 5.832 | 56.4 | 1.517 |
| PdI: | 0.286 | Peak 2: | 112.0 | 31.9 | 53.80 |
| Intercept: | 0.760 | Peak 3: | 4822 | 7.4 | 718.2 |

**Result quality :** Refer to quality report

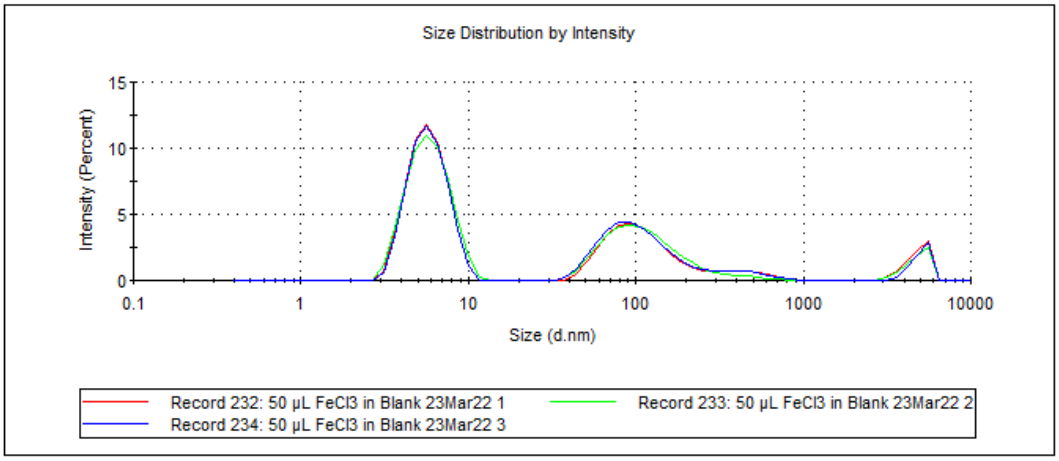


Figure 17. DLS of solvent with $FeCl_3$ (3.75 mM).

| | | Size (d.nm): | % Intensity: | St Dev (d.nm): |
|---|---|---|---|---|
| Z-Average (d.nm): 259.3 | Peak 1: | 6.322 | 34.7 | 1.173 |
| PdI: 0.777 | Peak 2: | 132.9 | 27.5 | 39.31 |
| Intercept: 0.833 | Peak 3: | 5091 | 20.0 | 557.4 |

**Result quality :** Refer to quality report

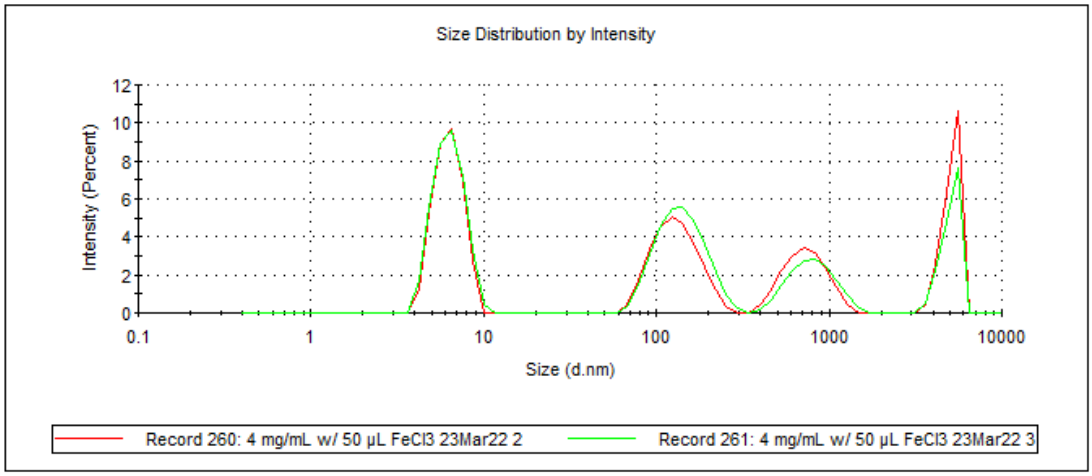


Figure 18. Carbamothioate (11 mM) with $FeCl_3$ (3.65 mM).

| | | Size (d.nm): | % Intensity: | St Dev (d.nm): |
|---|---|---|---|---|
| Z-Average (d.nm): 35.36 | Peak 1: | 86.25 | 62.5 | 39.78 |
| PdI: 0.669 | Peak 2: | 6.003 | 26.7 | 1.381 |
| Intercept: 0.825 | Peak 3: | 538.1 | 6.7 | 191.1 |

**Result quality :** Refer to quality report

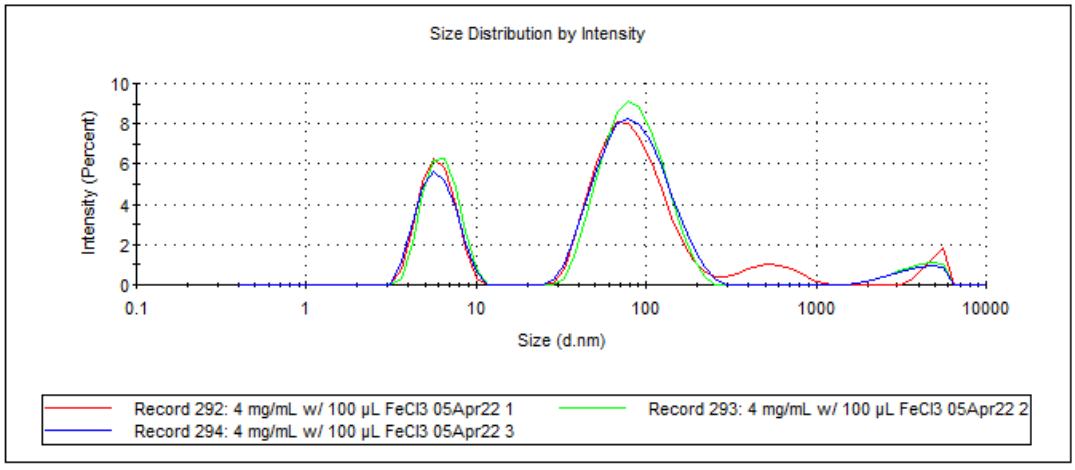


Figure 19. Carbamothioate (11 mM) with $FeCl_3$ (7.14 mM).

## 4.0 Future Work

Now that it's been shown that the carbamothioate is most active in the presence of $Fe^{3+}$ and with a transmembrane potential, the next step will be to see how the compound works with cells in vitro. Cell viability assays will be performed by dosing cells of a similar transmembrane potential to that of *Plasmodia* with the carbamothioate and cotreatment with $FeCl_3$ at varying concentrations and without any $FeCl_3$ at all. If cells remain viable in the presence of compound and no $FeCl_3$ but show substantial cell death in those treated with both, then that would provide evidence of the selectivity of our compound. Furthermore, by running various viability assays at different $FeCl_3$ concentrations, one could then determine the "lethal" amount of $FeCl_3$ required. Ideally this would be within the iron concentrations of erythrocytes that have an active malaria parasitic infection. However, if the iron requirements are too high and aren't physiologically relevant, the next step would be to increase the active concentration of the compound without having to increase the dose. This may be achieved by linking two or more carbamothioate molecules onto one linker molecule. A proposed reaction would be the Williamson ether synthesis reacting a linker molecule with multiple hydroxyl groups such as propylene glycol, and base to perform two $S_N2$ reactions on the bromine of each compound to link them together. A proposed reaction is presented in Figure 20 with propylene glycol. However, there are many options that may be explored to best optimize the compounds effectiveness.

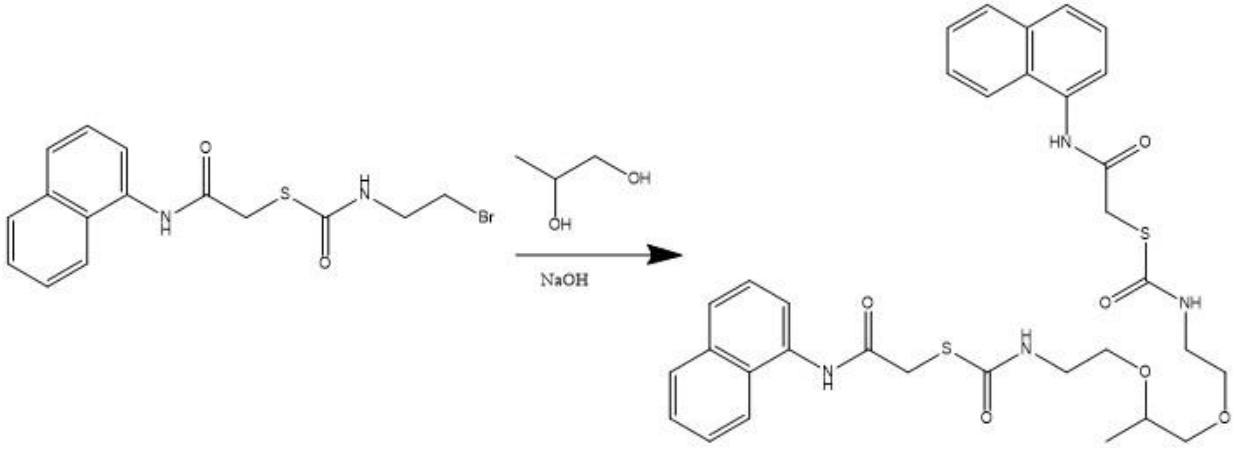


Figure 20. Proposed synthetic route with propylene glycol.

## 5.0 Conclusion

The need for a new type of antimalaria therapeutic is without question. In this work we've shown that the novel compound carbamothioate possesses unique properties that allow it to target an infected erythrocyte. The conditions in which our compound is active should only be present within an actively infected erythrocyte conferring great specificity. We've demonstrated not only a dose dependent response, but a response that is maximized when there is a negative transmembrane potential and free $Fe^{3+}$. Due to the unique structure of our compound, drug resistances found in *Plasmodia* populations would not likely confer resistance to this compound. Furthermore, the formation of micelle in aqueous media could also be used to this drugs advantage. Micelles lower the working concentration of a circulating drug thus lowering potential off-target toxicities and can deliver a more concentrated dose when the right conditions are met. In conclusion, in this work we present a novel anti-malarial therapeutic with great potential.

References


[1] World Health Organization. (2021, Dec 6). "*Malaria*" https://www.who.int/news-room/fact-sheets/detail/malaria

[2] Strode C, Donegan S, Garner P, Enayati AA, Hemingway J. *The impact of pyrethroid resistance on the efficacy of insecticide-treated bed nets against African anopheline mosquitoes: systematic review and meta-analysis*. PLoS Med 2014; 11: e1001619

[3] *RTS,S Clinical Trials Partnership. Efficacy and safety of RTS,S/AS01 malaria vaccine with or without a booster dose in infants and children in Africa: final results of a phase 3, individually randomized, controlled trial*. Lancet 2015; **386**: 31–45.

[4] Neafsey DE, Juraska M, Bedford T, et al. *Genetic diversity and protective efficacy of the RTS,S/AS01 malaria vaccine*. N Engl J Med 2015; **373**: 2025–37.

[5] Rodrigues, C.D., Jahn-Hofmann, K., et al. *Host scavenger receptor SR-BI plays a dual role in the establishment of malaria parasite liver infection*. Cell Host Microbe 2008; 4, 271–282.

[6] Greenberg, A. E., et al. *Hospital-based surveillance of malaria-related paediatric morbidity and mortality in Kinshasa, Zaire.* Bull World Health Organization Supplement 1989: **67**: 189-196

[7] Nguyen-Dinh, P. et al. *Plasmodium falciparum in Kinshasa, Zaire: in vitro drug susceptibility studies.* American Journal of Tropical Medicine and Hygiene. 1987: **37**: 217-219

[8] Roper, C. et al. *Antifolate antimalarial resistance in southeast Africa: a population-based analysis.* The Lancet 2003: **361**: 1174-1181

[9] Goldberg, D. E. (2005). Hemoglobin Degradation. In *Malaria: Drugs, disease and post-genomic biology* (pp. 275–287). essay, Springer.

[10] Sherman, I.W., Tanigoshi, L. *Incorporation of 14C-Amino-Acids by malaria (plasmodia lophurae) IV. In vivo utilization of host cell haemoglobin.* Int J. of Biochem. 1970; **1**: 635-637

[11] Ginsberg, H. *Some reflections concerning host erythrocyte-malarial parasite interrelationships.* Blood Cells 1990: **16**: 225-35

[12] Lew, V.G., Tiffert, T., Ginsberg, H. *Excess hemoglobin digestion and the osmotic stability of Plasmodium falciparum-infected red blood cells.* Blood 2003: **101:** 4189-94

[13] Egan, T. J. *Physico-chemical aspects of hemozoin (malaria pigment) structure and formation*. Journal of Inorganic Biochemistry 2202: **91**: 19-26

[14] Vurchow, R. *Zur pathologischen Physiologie des Bluts*. Archiv f. pathol. Anat 1847: **1**: 547-563

[15] Egan, T.J., Masuvo, W. W., Ross, D.C., Marques, H.M. *Thermodynamic factors controlling the interaction of quinoline antimalarial drugs with ferriprotoporphyrin IX.* Journal of Inorganic Biochemistry 1997: 68**: 137-145**

[16] Surolia, N., Padmanaban, G. *De novo biosynthesis of heme offers a new chemotherapeutic target in the human malarial parasite* Biochem Biophys Res Commun. 1992: **187**: 744-750

[17] Clark, M., Fisher, N.C., Kasthuri, R., Hand, C.C. *Parasite maturation and host serum iron influence the labile iron pool of erythrocyte stage Plasmodium falciparum.* British Journal of Heamotology 2019: **161**: 262-269

[18] Mabeza, G.F., Loyevsky, M.L., Gordeuk, V.R., Weiss, G. *Iron Chelation Therapy for Malaria: A Review* Pharmacology & Therapeutics 1999: **81**: 53-75

[19] Allen, R. J.W., Kirk, K., *The Membrane Potential of the Intraerythrocytic Malaria Parasite Plasmodium falciparum.* JBC 2004: **279**: 11264-11272

[20] Zavodnik, I. B. et al. *Human red blood cell membrane potential and fluidity in glucose solutions.* Scandanavian Journal of Clinical and Laboratory Investigation 1997: **57**: 59-63

[21] Li, H. et al. *Graphene field effect transistors for highly sensitive and selective detection of $K^+$ ions.* Sensors and Actuators B: Chemical 2017: **253**: 759-765

[22] Akerman, K., E., Wikstrom, M., K. *Safranine as a probe of the mitochondrial membrane potential.* FEBS Letters 1976: **68**: 191-197

[23] Franklin, C., D. *A Controlled Cyclization of Functionalized Thioureas and Unprecedented Termolecular Decyclization of Iminothiazolidinones.* Chemistry Select 2019: **4**: 3567-3576

[24] Stetefeld, J. et al. *Dynamic light scattering: a practical guide and applications in biomedical sciences.* Biophysical Reviews 2016: **8**: 409-427